Sustainable Engineering Materials
ISSN: waiting (Print); ISSN: waiting (Online)
http://www.sustain-dpl.com/picnews.asp?id=177
DOI: 10.54113/j.suem.2026.000022

ORIGINAL ARTICLE

Effect of material imperfections on thermal behavior in metal matrix composites: a finite element approach

Md. Shakil Al Kajem Mondal, Md. Abdul Hasib*, Arup Kumar Debnath, Al Muttaki Billah, Dipayan Mondal, Md. Ashraful Islam

Department of Mechanical Engineering, Khulna University of Engineering and Technology, Khulna-9203, Bangladesh
*Corresponding Author: Md. Abdul Hasib. Email: ahasib@me.kuet.ac.bd

Abstract: This study examines the thermal stress behavior of metal matrix composites (MMCs), with a focus on the influence of voids on thermal strain and the coefficient of thermal expansion (CTE). A finite element model (FEM) was developed using the software ABAQUS to simulate the thermal behavior of MMCs with ceramic particle reinforcement and to compare the models with and without voids using a two-dimensional periodic unit cell approach. The results showed that voids significantly increased thermal strain. At 473 K, the presence of voids increased the thermal strain by 8.50% in Model 1 and 2.27% in Model 2 compared with their corresponding void-free configurations. Additionally, the composite with voids exhibited a higher CTE, confirming that microstructural flaws impact thermal behavior. The thermal stress response of the composite with voids was about 15% higher than that of the control samples, underlining how voids affect the composite's thermal behavior. These results show the need to model material imperfections, including voids, accurately when determining the thermal performance of composites. The findings provide valuable insights for optimizing the design and reliability of MMCs, particularly in applications where thermal behavior is critical, such as in aerospace, automotive, and energy industries.

Keywords: metal matrix composites, thermal stress, finite element analysis, coefficient of thermal expansion

1 Introduction

Composite materials are renowned for being light, strong, and corrosion-resistant. Aerospace, automotive, electronics, and energy sectors rely on these materials to boost efficiency and enable complex designs. Notably, combining different materials for better performance is not a new concept: ancient artisans laminated wood into early plywood and reinforced clay bricks with straw [1]. The advent of synthetic polymer matrices and advanced reinforcements has revolutionized composites, driven by aerospace's demand for weight reduction without sacrificing strength [2]. Among composite classes, metal matrix composites (MMCs) reinforced with ceramic particles have become vital in high-temperature, high-stress environments for their high stiffness, wear resistance, and thermal resilience. Magnesium alloy-based MMCs like AZ91D offer an excellent stiffness-to-weight ratio along with corrosion resistance and effective heat dissipation, making them integral to aerospace and automotive applications [3].

However, the advantages of MMCs can be undermined by material imperfections like internal voids, uneven reinforcement dispersion, and thermal expansion mismatches between matrix and

Received: 24 November 2025; Received in revised form: 14 August 2026; Accepted: 14 August 2026

particles. To address these challenges, researchers have increasingly turned to finite element modeling (FEM) to simulate thermal stress responses and guide composite design optimization, and extensive studies have examined the mechanical and thermal behavior of MMCs in recent decades. Aluminum- and magnesium-based MMCs with ceramic reinforcements can outperform conventional alloys. Chang et al. [4] laid the groundwork for systematic studies of thermal effects in composites, highlighting the crucial impact of matrix–reinforcement CTE mismatches on internal stresses (large mismatches can induce debonding or even catastrophic failure). Since then, researchers have used micromechanical modeling and FEA to probe these issues. For example, multiple studies [5-10] employed analytical and numerical approaches to examine how microstructural factors influence thermal stress development, modeling thermal expansion behavior remains an active focus: Lvov and Tănase [11] explored plastic deformation mechanisms under elevated temperatures; Bai et al. [12] performed meso-scale FEA of composite responses under complex loading; Bouchara et al. [13] analyzed crack propagation under combined thermal–mechanical loads; and Bahl and Bagha [14] simulated fiber–matrix debonding.

Microstructural features can also affect composite performance. Precipitate-free zones around reinforcement particles can alter local stress distributions during thermal cycling [15], while multiscale modeling links nanoscale phenomena to macroscale behavior [16]. The thermal response of an MMC is further influenced by interfaces and porosity. Nam et al. [17] found that in densely packed SiC-Al composites, the effective CTE drops when voids are present. Similarly, interface thermal resistance and residual stresses can significantly affect overall thermal behavior [18, 19]. Different reinforcement types and heat treatments can also alter a composite's thermal expansion and wear properties [20, 21]. Additive manufacturing processes introduce their own thermal effects: Mirkoohi et al. [22] modeled the thermal stresses induced by metal additive manufacturing, underscoring the importance of capturing realistic thermal gradients; Shen [23] similarly argued that both void content and phase continuity must be included for accurate thermal expansion modeling. To achieve higher fidelity, several studies [24-27] have incorporated realistic particle shapes, size distributions, and microstructural images into FEA, significantly improving simulation fidelity. Collectively, this body of work shows that accurate modeling of composite thermal behavior requires not only proper material selection but also careful consideration of internal flaws, interface effects, and thermal loading conditions.

The foundations of composite thermomechanical modeling were established in the 1980s and 1990s with idealized micromechanical models [28, 29]; by the late 1990s periodic unit cell models and X-ray CT data [30] demonstrated the strong influence of matrix–particle CTE mismatch on internal stresses. In the 2000s, microstructure-informed FEM techniques gained traction: 2D cross-sectional FEM models captured anisotropic composite behavior [31], and 3D X-ray tomography enabled image-based simulations with actual particle distributions and porosity [32, 33]. Interfacial debonding and damage in MMCs have been investigated through numerical modelling [34], including three-dimensional simulations of void nucleation and coalescence [35]. Cohesive-zone [36] and micromechanical models [37] have further been used to study crack propagation and interfacial failure. More recently, X-ray CT-informed FEA has enabled realistic assessment of particle clustering and damage initiation [38], while numerical studies have also examined thermal damage in particulate MMCs [39]. Despite these advancements, magnesium-based systems like AZ91D received far less attention than aluminum-based composites. Recent years have seen progress in modeling Mg-based MMCs. Hou et al. [40] applied a crystal-plasticity model to investigate thermal-mismatch-induced dislocations and twins in metal matrix composites, and Chen et al. [41] developed a finite-element model to investigate the mechanical response and damage behavior of Ti_2AlC-reinforced magnesium composites. High-fidelity image-based FEA incorporating real SiC particle geometries and embedded porosity revealed major reductions in mechanical performance when pores are clustered [42, 43]. Advances in additive manufacturing as laser powder bed fusion, now allow tailoring of internal composite structures: for example, adding nano-scale ceramic reinforcements reduced porosity and improved ductility in AZ91D-TiC composites [44], and FEM simulations help optimize process parameters for additively manufactured MMC components [45]. Furthermore, AI and data-driven techniques are augmenting modeling: deep learning image analysis has improved failure prediction [46], and machine learning-assisted FEM can predict thermal properties and residual stresses in near real-time [47, 48], enabling digital twins for predictive maintenance.

Despite these advances, a targeted FEM investigation into AZ91D-F/SiC composites incorporating voids and thermal loads across realistic service temperatures remains scarce. Most existing models overlook how even minor porosity influences thermal strain and CTE evolution. Furthermore, the combined effects of interface debonding and matrix expansion mismatch under cyclic heating are often excluded. In response, this work uses ABAQUS finite element simulations to examine how a small void content (0.25% vol) affects the thermomechanical behavior of AZ91D/SiC. Periodic unit cell models with and without voids are analyzed over 293-473 K to quantify changes in thermal strain, internal stress distribution, and effective CTE. By incorporating realistic microstructural features and applying coupled thermal-mechanical loads, this study bridges this modeling gap and informs the design of composites for demanding service conditions.

Although the thermal behavior of metal matrix composites has been extensively studied, the quantitative influence of micro-voids on the thermal strain, effective coefficient of thermal expansion (CTE), and thermoelastic stress distribution of AZ91D-F/SiC composites remains insufficiently understood. This study addresses this gap by comparing void-free and void-containing unit-cell models under identical thermal loading conditions to evaluate the effect of micro-voids on the thermal response and stress distribution of the composite.

2 Numerical Modeling

In this study, a two-unit cell models were developed to investigate the deformation behavior of metal matrix composites (MMCs) under thermal loading. These models capture the evolution of thermal stresses as the temperature rises from 293 K (20°C) to 473 K (200°C). Both employ an idealized two-dimensional unit-cell framework. The analysis is intended to compare the relative thermal response of void-containing and void-free configurations; therefore, the modeled void is interpreted as a through-thickness cylindrical defect within the two-dimensional representation. These models, which are depicted in **Fig. 1** and **Fig. 2**, were influenced from the model presented by Nam et al. [17]. **Fig. 1** shows the first unit cell model, which utilizes a square-shaped AZ91D-F matrix to simulate SiC contiguity. This setup ensures a realistic representation of the matrix-reinforcement interactions in the composite. **Fig. 2** presents the second model, a SiC network model, where 28 vol.% of the material is matrix, and the remaining volume is SiC particles.

This configuration was designed to further understand the role of reinforcement in the thermal behavior of the MMC. Both models were developed with and without voids to analyze the impact of material imperfections, specifically voids, on the thermal properties of the composite. Given the

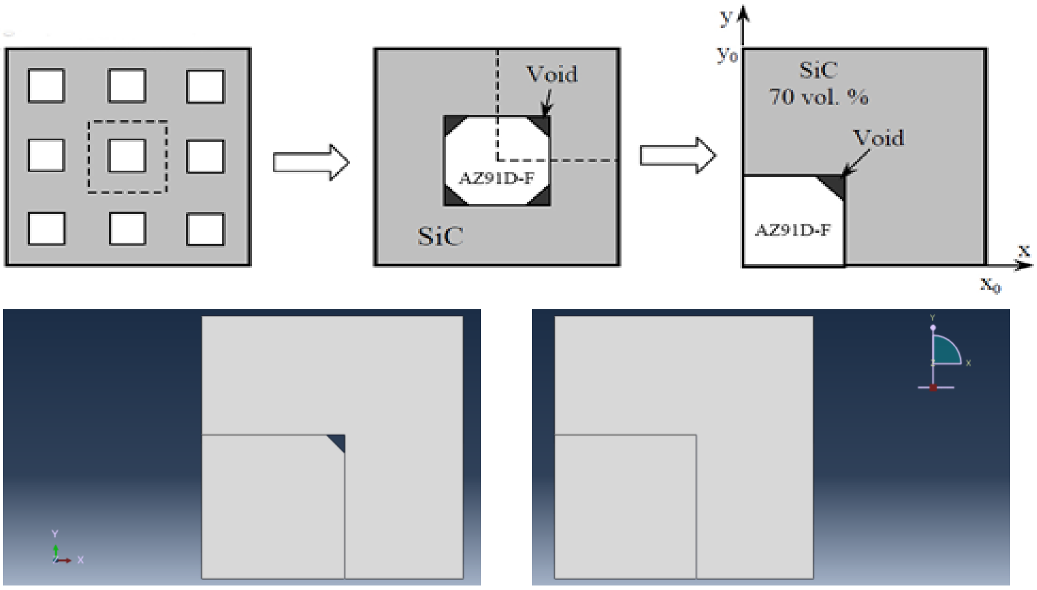

(a) (b)

Fig. 1. Two-dimensional phase arrangement with a microscopic void for model 1. (a) with void. (b) without void.

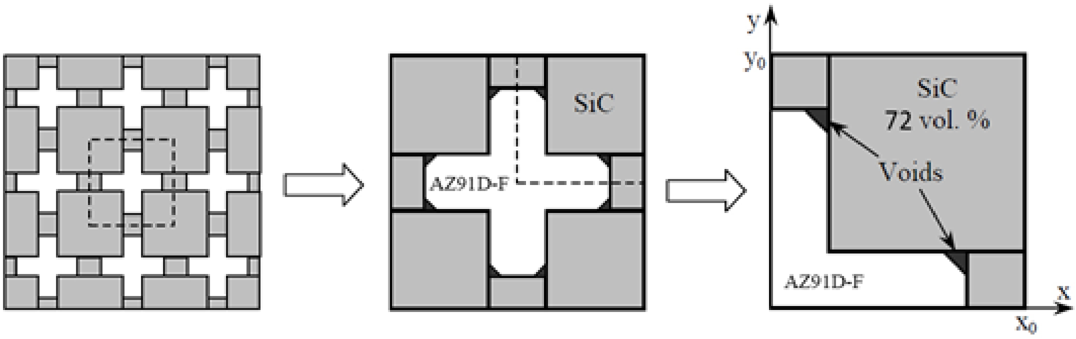

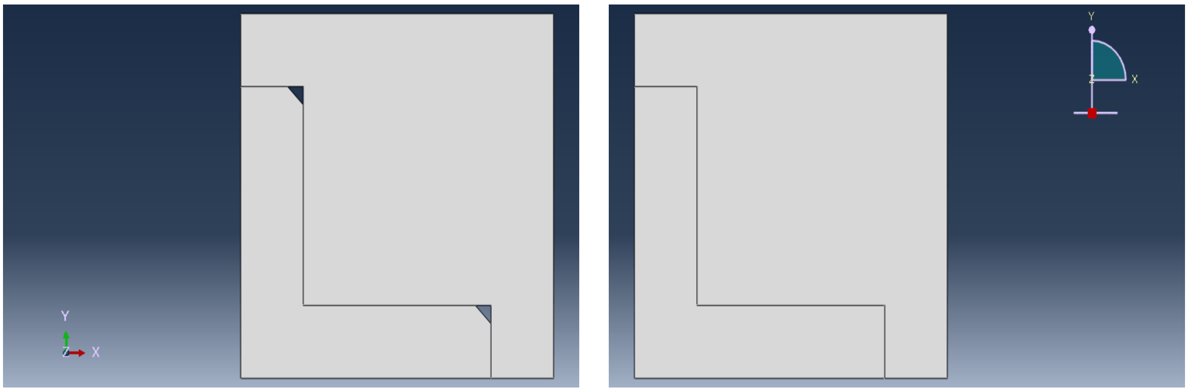

(a) (b)

Fig. 2. Two-dimensional phase arrangement with a microscopic void for model 2. (a) with a void. (b) without void.

symmetry of the unit cell, only a single quadrant of each model was used for simulation to reduce computational costs. In both models, the volume fraction of voids was assumed to be 0.25 vol.%, representing a moderate level of porosity in the material.

The material properties used in the models are summarized in **Table 1**, which lists the coefficient of thermal expansion (CTE), yield stress, Young's modulus, and Poisson's ratio for both the AZ91D-F matrix and SiC reinforcement. These values were taken from existing literature and reflect the temperature-dependent behavior of the materials. It is assumed that the AZ91D-F alloy and SiC particles are perfectly bonded, simplifying the interaction model between the two phases. The chemical composition of the AZ91D-F alloy is provided in **Table 2**, giving insight into the material's composition, which influences its thermal and mechanical properties.

Table 1. The Young's Modulus *E* (GPa), Poisson Ratio *v*, Yield Stress $\sigma_{0.2}$ (MPa), and CTE (μm/m.°C) of matrix and reinforcement for finite element modeling [49, 50]

AZ91D-F					SiC		
T (°C)	*E* (GPa)	*v*	CTE (μm/m.°C)	$\sigma_{0.2}$ (MPa)	*E* (GPa)	ν	CTE (μm/m.°C)
50	44.8	0.35	27.2	150	450	0.18	2.78
100	44.8	0.35	27.2	150	450	0.18	3.09
200	44.8	0.35	27.2	150	450	0.18	4.16

Table 2. Component Elements of Magnesium AZ91D-F [51]

Element	Content (%)	Element	Content (%)
Aluminum, AL	8.3 - 9.7 %	Manganese, Mn	>= 0.13 %
Copper, Cu	<= 0.030 %	Nickel, Ni	<= 0.0020 %
Iron, Fe	<= 0.0050 %	Silicon, Si	<= 0.10 %
Magnesium, Mg	90 %	Zinc, Zn	0.35 - 1.0 %

The numerical simulation was carried out under the assumption that all components start with zero stress at an initial temperature of 20°C. The entire model was then subjected to a uniform temperature increase of 200°C (from 293 K to 473 K), which was applied in ABAQUS through a temperature step. The thermal loading was chosen to represent typical operating conditions for MMCs in high-temperature environments. To establish a consistent reference frame, displacement constraints were applied along the left and bottom boundaries of each unit-cell model during the thermo-mechanical analysis. The same boundary conditions were maintained for all numerical models to enable a direct comparison between the void-free and void-containing configurations under identical thermal loading conditions. Although periodic boundary conditions provide a more rigorous representation of an infinitely repeating composite microstructure, the adopted boundary conditions were considered adequate for the comparative objective of the present study. This simplification may influence the absolute values of the predicted stresses and strains but is not expected to alter the relative trends observed between the investigated models. The bottom and left edges of the unit cell were fixed in displacement, preventing any motion at these boundaries, while the top and right edges were free to deform in response to thermal stress. The boundary conditions were set up carefully to reflect realistic constraints and allow the model to behave as it would in a physical scenario.

The CTE values listed in **Table 1** represent mean coefficients of thermal expansion over the investigated temperature range and were adopted directly from the referenced experimental data. The material properties used in the finite element analysis are summarized in Table 1. The temperature-dependent material properties of AZ91D-F were adopted from the ASM Handbook and the ASM Specialty Handbook: Magnesium and Magnesium Alloys [49,50]. The CTE values represent the mean coefficients of thermal expansion over the corresponding temperature ranges and were considered appropriate for the present comparative analysis.

For meshing, unit cell model 1 was meshed with 11,578 elements for the configuration with voids and 11,540 elements for the configuration without voids, ensuring that the mesh density was sufficient to accurately capture the thermal stress distribution. Unit cell model 2 was meshed with 11,660 elements. The chosen element count strikes a balance between computational efficiency and the fidelity of the model. The mesh resolution remains sufficient to capture stress concentrations around voids and along matrix–reinforcement interfaces.

2.1 Mesh Sensitivity Analysis and Accuracy Verification

For the numerical analysis, a 3-node triangular element (CPS3) in Abaqus was used to mesh the matrix and SiC particles within the unit cell models. This element type captures thermal and mechanical responses efficiently. For Unit Cell Model 1, the mesh contained 11,578 elements with voids and 11,540 without them. Unit Cell Model 2 had 11,660 elements. Our mesh sensitivity analysis guided us to make a choice of element numbers, balancing accuracy with computational time and cost.

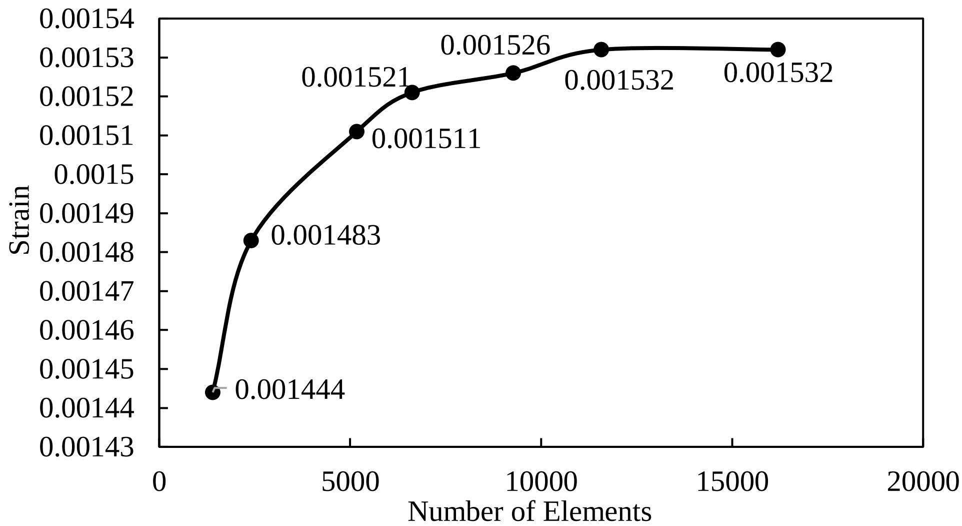

Fig. 3. Mesh sensitivity analysis showing the variation of strain for different numbers of elements.

Fig. 3 presents how strain at 473 K changes with different mesh densities. The strain shifts quickly when the element count rises from 1,000 to 7,000, reflecting a clear improvement in accuracy in this range. However, beyond 10,000 elements, further changes in strain become minor. At around 11,578elements, results stabilize, showing negligible differences compared to simulations using 16,203 elements. This means increasing the count past 11,578 offers little accuracy gain but raises computational demand. Thus, 11,578 elements were identified as optimal, providing accuracy while reducing computation time and memory load. The present analysis employed CPS3 linear triangular elements for all numerical models because they provide robust discretization of the representative unit-cell geometries while maintaining numerical stability. The same element type and mesh strategy were adopted consistently for all simulations to enable a direct comparison of the influence of micro-voids under identical modeling conditions. The mesh convergence study demonstrated that the predicted thermal strain became essentially mesh-independent beyond approximately 11,500 elements, indicating that the adopted discretization is adequate for the comparative objectives of this study. Although higher-order or quadrilateral elements may improve the prediction of localized stresses near geometric discontinuities, this aspect was beyond the scope of the present comparative investigation and will be considered in future work.

To validate the accuracy of the simulation results, a comparison was made with previously published work by T.H. Nam [17]. The published data were extracted using Plot Digitizer for a direct check. **Fig. 4** shows strain against temperature, comparing the current results with Nam's data. The agreement between the two sets is clear, with only a small margin of error. This minimal discrepancy further supports the validity of the modeling approach used in this study, confirming that the numerical simulation method is both accurate and reliable for predicting the thermal stress behavior of metal matrix composites.

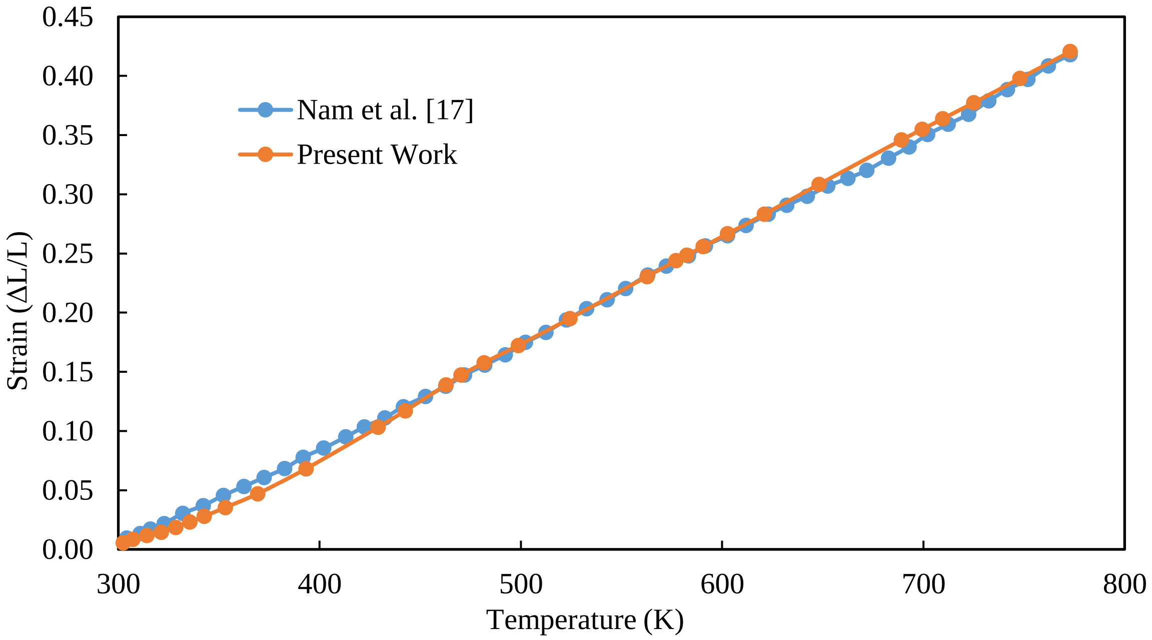

Fig. 4. Comparative analysis of strain variation at different temperatures, including the Present work versus Nam's study.

Although good agreement is observed between the numerical and experimental results, minor discrepancies are expected because the finite element model employs several simplifying assumptions. The model considers idealized reinforcement geometry, perfect matrix–particle interfacial bonding, homogeneous material properties, and a linear thermoelastic constitutive response. In contrast, the experimental material contains unavoidable manufacturing-induced imperfections, local microstructural heterogeneity, residual stresses, and interfacial defects that are not explicitly represented in the simulation. These factors contribute to the observed differences while remaining within an acceptable range for validating the present comparative numerical model.

3 Results and Discussions

The Finite Element Analysis (FEA) was conducted using Abaqus to investigate the thermal expansion behavior of SiC-reinforced AZ91D-F matrix composites under thermal loading. The unit cell models were subjected to a uniform temperature change, increasing from 293 K (20°C) to 473 K (200°C). As the temperature rose, displacement occurred within the model, with the displacement contours showing the largest shifts in specific regions. These displacement patterns are shown in **Fig. 5**, where the highest displacement is highlighted in red. It is clear from the figure that the corners of both the matrix and SiC reinforcement experienced the greatest displacements, which is consistent with the expected behavior of materials under thermal expansion, particularly where there are sharp geometric angles or interfaces. As expected, thermal strains developed as the temperature of the unit cell model increased. These strains are typically linear in nature, meaning the strain increases proportionally with temperature. The micro-voids were intentionally placed at the matrix–reinforcement interface, where thermal stresses are expected to be highest because of the mismatch in elastic modulus and coefficient of thermal expansion between the matrix and reinforcement. Thus, the predicted stresses represent the combined effects of the void and the corner geometry. Future work will investigate the influence of different void locations.

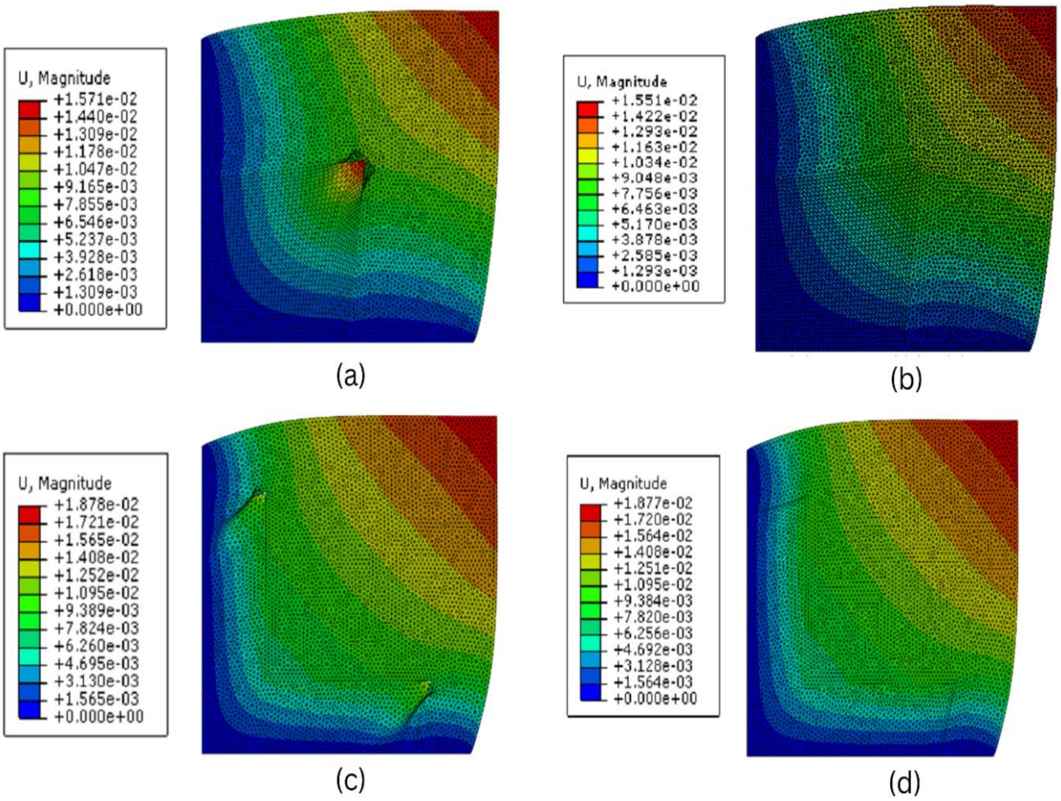

Fig. 5. Physical displacement contour at 473 K for (a) Model 1(A), (b) Model 1(B), (c) Model 2(A), and (d) Model 2(B)

Fig. 6 illustrates the thermal strain distribution at 473 K for the four unit-cell models. The maximum thermal strain is concentrated near the matrix–reinforcement interfaces and geometric discontinuities, where the mismatch in thermal expansion behavior between the AZ91D-F matrix and SiC reinforcement generates localized deformation. The strain contours further indicate that the models containing micro-voids exhibit slightly higher thermal strain than their corresponding void-free counterparts. This increase is primarily attributed to the reduced local stiffness introduced by the voids, which allows greater thermal deformation under identical thermal loading conditions. **Fig. 7** presents the variation of thermal strain with temperature for all four models. As expected, thermal strain increases continuously with increasing temperature due to the thermal expansion of the constituent materials.

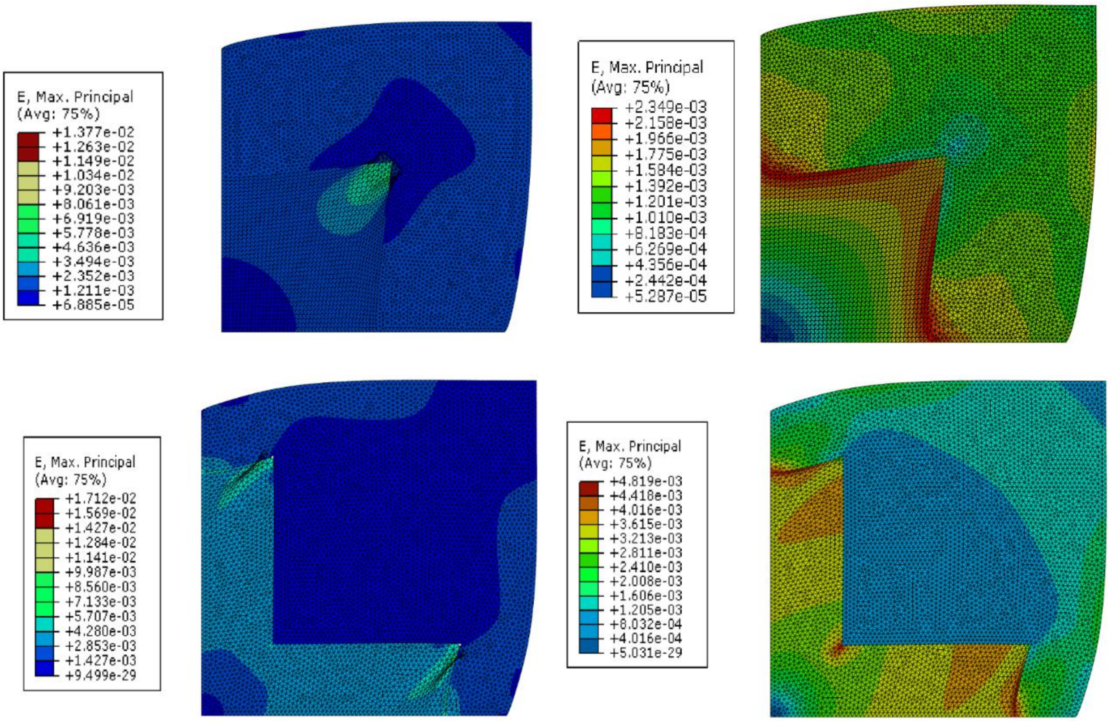

Fig. 6. Thermal strain contour at 473 K using Model 1(A), Model 1(B), Model 2(A), and Model 2(B) (Left to Right).

A comparison between the void-containing and void-free models shows that the presence of voids leads to a higher overall thermal strain response. This behavior can be attributed to the reduction in effective stiffness caused by the voids. The voids act as local compliance regions that allow the surrounding matrix material to deform more freely under thermal loading. Consequently, the composite exhibits greater thermal deformation than the corresponding void-free model.

At 473 K, Model 1(A) exhibited a thermal strain of 1.532×10^{-3} compared to 1.412×10^{-3} for Model 1(B), while Model 2(A) showed a thermal strain of 1.939×10^{-3} compared to 1.896×10^{-3} for Model 2(B). These results confirm that the incorporation of micro-voids increases the global thermal strain of the composite. Furthermore, the thermal expansion mismatch between the AZ91D-F matrix and SiC reinforcement promotes localized stress redistribution around the void boundaries, reducing local

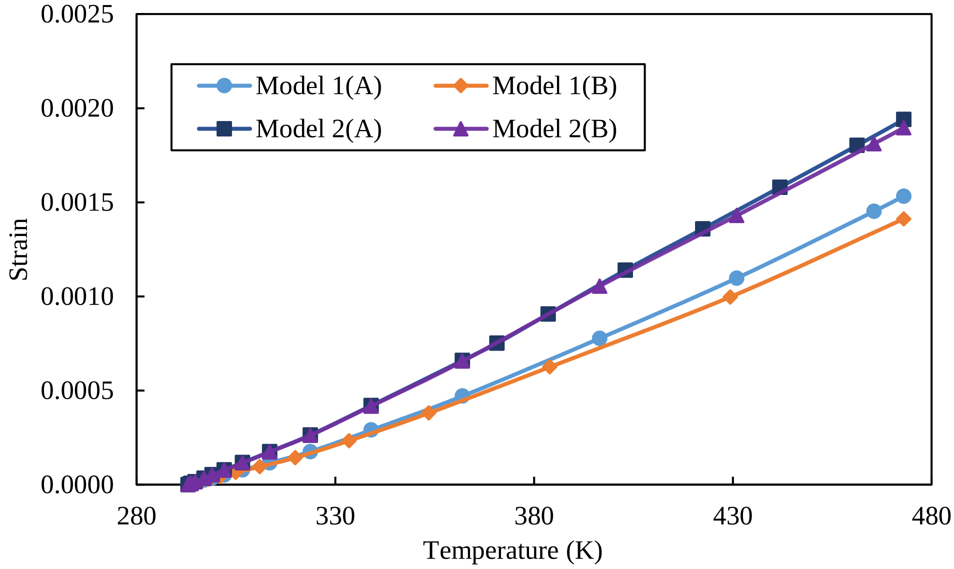

Fig. 7. Comparison of thermal strain of four models with temperature change.

constraints on matrix expansion and contributing to the observed increase in thermal strain. Based on these values, the presence of the micro-void increased the thermal strain by approximately 8.50% in Model 1 and 2.27% in Model 2 relative to the corresponding void-free configurations. The influence of voids is more pronounced in Model 1 than in Model 2, indicating that the effect of porosity on thermal deformation also depends on the reinforcement topology and matrix continuity within the unit-cell structure.

The Von Mises equivalent stress distribution, as illustrated in **Figs. 8(a) and 8(b)** indicate that the maximum thermal stress consistently develops at the corners of both the matrix and SiC reinforcement for Model 1(A) and Model 1(B). In Model 2(A) and Model 2(B), shown in **Figs. 8(c) and 8(d)**, the maximum stress shifts to the corners of the SiC reinforcement, especially in areas where the contrast in material properties between the matrix and reinforcement is the most pronounced. This localized stress concentration is typical in composite materials, where differences in the thermal expansion properties of the matrix and reinforcement lead to stress build-up, particularly at sharp corners or interfaces.

The presence of the micro-void reduces the effective stiffness of the composite, allowing greater overall thermal deformation under identical thermal loading. At the same time, the void alters the local load-transfer mechanism and redistributes the principal strain field around the defect and the matrix-reinforcement interface. Consequently, the strain concentration is redistributed spatially rather than uniformly reduced, while the overall thermal strain of the composite increases.

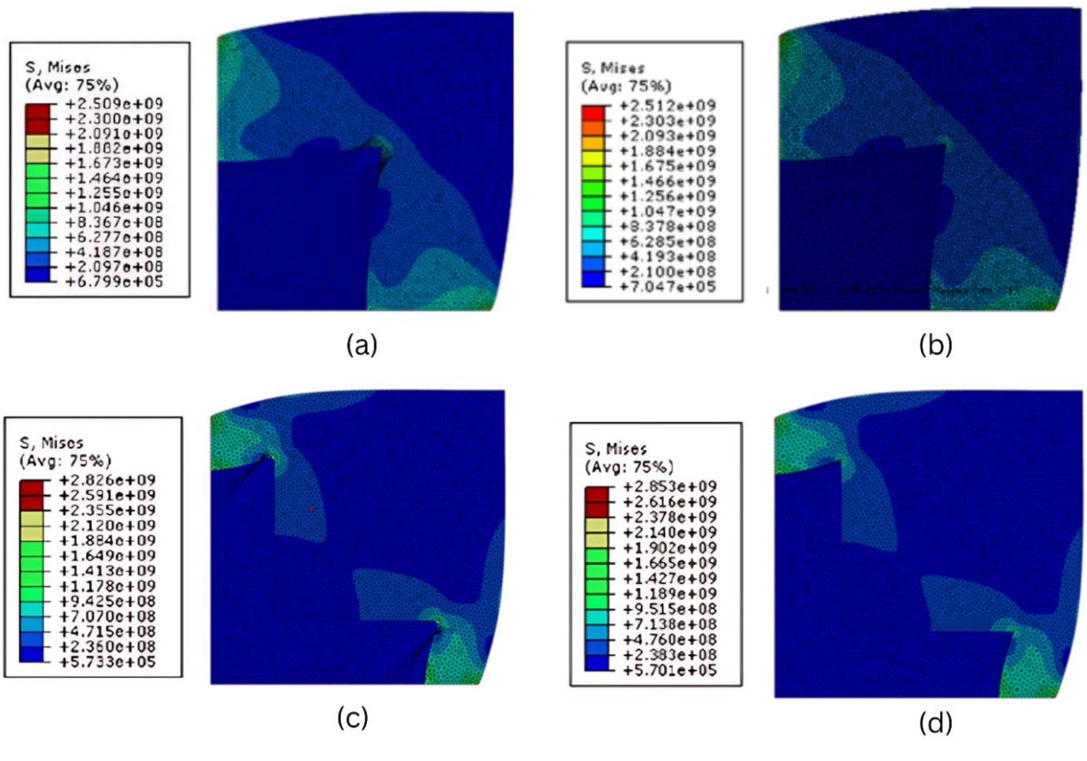

Fig. 8. Mises equivalent stress distribution at 473 K using (a) model 1(A), (b) model 1(B), (c) model 2(A), and (d) model 2(B)

The highest stresses are observed near the corners of the SiC reinforcement. This behavior results from the combined effects of the mismatch in elastic modulus and coefficient of thermal expansion between the AZ91D-F matrix and the SiC particles. During heating, the matrix attempts to expand more than the relatively stiff reinforcement, producing localized thermal stresses at the bonded interface. The sharp corners of the square SiC particles further amplify these stresses because of geometric stress concentration, resulting in the maximum stress occurring at these locations.

Moving to the Coefficient of Thermal Expansion (CTE), **Fig. 9** compares the CTE of the four-unit cell models as the temperature increases. The analysis shows a general rise in CTE across all models,

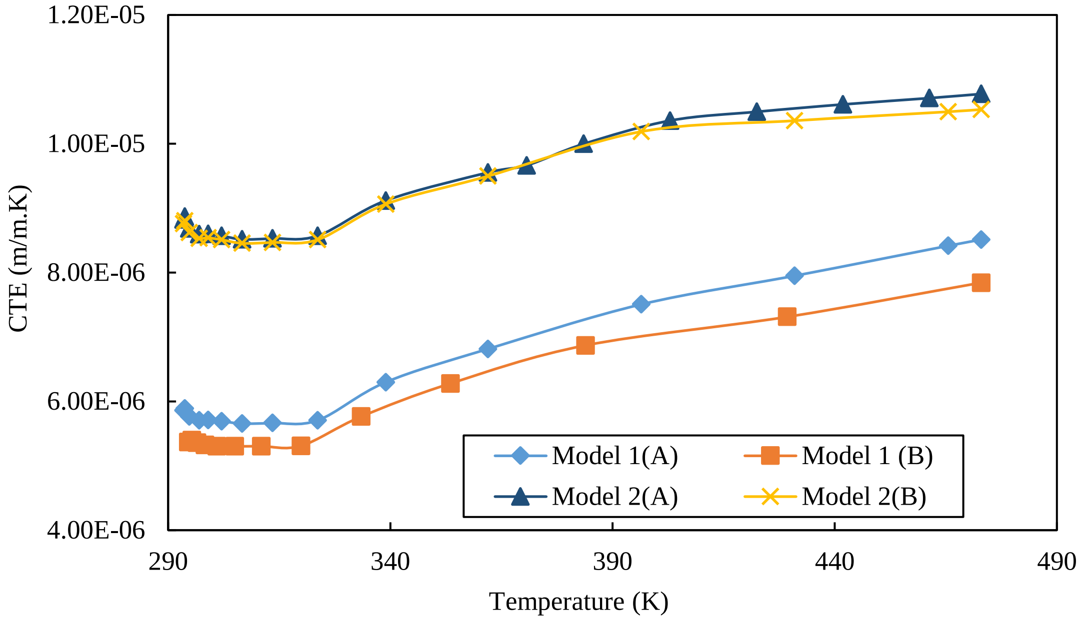

Fig. 9. Comparison of CTE versus temperature for 4 different models

with a slight dip at lower temperatures, which is typical for many composite materials. However, the CTE for Model 2(A) was slightly higher compared to Model 2(B), and similarly, Model 1(A) showed a higher CTE than Model 1(B) at corresponding temperatures. These differences in CTE can be attributed to slight variations in material distribution and possibly the reinforcement volume in the models, particularly in Model 2, where the distribution of SiC particles or the presence of voids can allow for more expansion.

The results show that micro-voids influence both the global and local thermal response of the composite. Compared with the void-free models, the void-containing models exhibited higher thermal strain and effective CTE. High stress concentrations were observed near the corners of the SiC reinforcement because of the mismatch in thermal expansion and elastic properties between the matrix and reinforcement. The voids also redistributed the local stress field, producing localized stress concentrations around the void boundaries. These results highlight the importance of controlling porosity to improve the thermomechanical performance of AZ91D-F/SiC composites.

The present analysis employs a linear thermoelastic constitutive model; therefore, plastic deformation and equivalent plastic strain (PEEQ) were not considered. Accordingly, the predicted von Mises stresses represent thermoelastic stress distributions and are used to compare the relative influence of micro-voids under identical modeling conditions. A temperature-dependent elasto-plastic constitutive model would provide a more realistic description of post-yield behavior and residual stresses and will be considered in future work.

3.1 Limitations of the Two-Dimensional Unit-Cell Representation

The present model uses a two-dimensional unit-cell representation to enable an efficient comparative assessment of the thermal response of void-containing and void-free AZ91D-F/SiC composites. Under this assumption, the modeled void represents a through-thickness cylindrical defect rather than an isolated spherical pore. Consequently, the predicted local stress and strain fields should be interpreted as two-dimensional approximations and may differ in magnitude from those associated with real three-dimensional pores.

In practical metal matrix composites, pores may be spherical, elongated, irregular, or interconnected, while the SiC reinforcement may exhibit three-dimensional connectivity and non-uniform spatial distribution. These features can influence local stiffness, stress redistribution, and thermal deformation. Therefore, the present results are most appropriate for identifying the relative influence of voids and reinforcement topology under consistent modeling conditions, rather than providing an exact representation of all real microstructural defects. Future work should employ three-dimensional representative volume element models incorporating spherical or experimentally measured pore geometries, realistic particle distributions, and interface behavior to quantify these effects more accurately.

4 Conclusions

We employed Abaqus FEA to investigate the thermal expansion behavior of SiC-reinforced AZ91D-F matrix composites. Our findings show that thermal strain rises as temperature increases. We observed that voids in the composite lead to notably higher strain and thermal stress. At 473 K, the thermal strain increased by 8.50% in Model 1 and 2.27% in Model 2 when the void-containing configurations were compared with their corresponding void-free models. Thermal stress was also higher in the void-containing models. These results highlight how even small imperfections can greatly impact thermal performance. We also found that displacement within the unit cell is not uniform. The highest displacement occurs at the unbounded corners. This observation confirms that voids affect how stress and strain spread across the composite. Thermal stress distribution maps provided further clarity. Stress rises sharply with temperature, especially in composites with voids. This behavior could affect performance when the material is exposed to real-world thermal conditions. These insights reveal the critical role of microstructural defects in shaping the thermal behavior of MMCs. Understanding these effects helps us design more reliable composites for aerospace, automotive, and energy applications where thermal stability is essential. This study underlines the need to model imperfections carefully so we can predict material behavior accurately and ensure dependable performance in practice.

Funding Statement

The author(s) received no specific funding for this study.

CRediT authorship contribution statement

Md. Shakil Al Kajem Mondal: Conceptualization, Methodology, Formal Analysis, Investigation, Visualization, Writing – original draft. **Md. Abdul Hasib:** Conceptualization, Methodology, Visualization, Supervision, Writing – review & editing. **Arup Kumar Debnath:** Conceptualization, Methodology, Writing – review & editing. **Al Muttaki Billah:** Investigation, Visualization, Writing – review & editing. **Dipayan Mondal:** Investigation, Data Curation, Writing – review & editing. **Md. Ashraful Islam:** Resources, Formal Analysis, Writing – review & editing.

Conflicts of Interest

The authors declare that they have no conflicts of interest to report regarding the present study.

Data Availability Statement

Some or all data, models, or codes that support the findings of this study are available from the corresponding author upon reasonable request.

References

[1] C. H. Strand, "Mechanical and impact tests of CFRP. An experimental and numerical study of the mechanical properties of CFRP samples with varying temperatures, using Four-point bending, Charpy and Air gun tests," UiT The Arctic University of Norway, 2017.
[2] R. R. Nagavally, "Composite materials-history, types, fabrication techniques, advantages, and applications," International Journal of Mechanical and Production Engineering 2017; 5(9): 82-87.
[3] S. A. A. Alem, "Advancing the next generation of high-performance metal matrix composites through metal particle reinforcement," Advanced Composites and Hybrid Materials 2025; 8(1): 3. https://doi.org/10.1007/s42114-024-01057-4
[4] C. Chang, "Thermal effects on polymer composites and metal matrix composites," Theoretical and Applied Fracture Mechanics 1987; 8(1): 49-57. https://doi.org/10.1016/0167-8442(87)90018-8
[5] H. Qing and T. Liu, "Micromechanical analysis of SiC/Al metal matrix composites: Finite element modeling

and damage simulation," International Journal of Applied Mechanics 2015; 7(2): 1550023. https://doi.org/10.1142/S1758825115500234

[6] C. Hung and S. Kobayashi, "Finite element deformation analysis of metal matrix composites," International Journal of Machine Tools and Manufacture 1992; 32(4): 601-617. https://doi.org/10.1016/0890-6955(92)90049-M

[7] S. Gatea, T. Jwad, F. Chen, and H. Ou, "Micromechanical modeling of the deformation and damage behavior of Al6092/SiC particle metal matrix composites," Journal of Materials Engineering and Performance 2023; 32(23): 10680–10701. https://doi.org/10.1007/s11665-023-07907-4

[8] W. Węglewski, "Finite element modeling of thermal residual stresses in functionally graded aluminum-matrix composites using X-ray micro-computed tomography," Finite Elements in Analysis and Design 2024; 241: 104239. https://doi.org/10.1016/j.finel.2024.104239

[9] R. A. González-Lezcano and J. M. del Río-Campos, "Numerical analysis of the influence of particle population characteristics in a metal matrix composite material," Journal of the Brazilian Society of Mechanical Sciences and Engineering 2023; 45(9): 457.

[10] M. Maździarz and S. Nosewicz, "Atomistic investigation of deformation and fracture of individual structural components of metal matrix composites," Engineering Fracture Mechanics 2024; 298: 109953. https://doi.org/10.1016/j.engfracmech.2024.109953

[11] G. Lvov and M. Tănase, "Numerical Modeling of Plasticity in Metal Matrix Fiber Composites," Applied Sciences 2024; 14(19): 8679. https://doi.org/10.3390/app14198679

[12] R. Bai, "Finite element analysis of mechanical behavior for SiC nanowires reinforced al matrix composites," Applied Composite Materials 2024; 31(2): 611-644. https://doi.org/10.1007/s10443-023-10188-8

[13] Z. Bouchra, "Finite element analysis of the thermomechanical behavior of metal matrix composites (MMC)," Fracture and Structural Integrity 2020; 14(51): 174-188. https://doi.org/10.3221/IGF-ESIS.51.14

[14] S. Bahl and A. K. Bagha, "Finite element modeling and simulation of the fiber–matrix interface in fiber reinforced metal matrix composites," Materials Today: Proceedings 2021; 39: 70-76. https://doi.org/10.1016/j.matpr.2020.06.160

[15] B. Lay and M. Boivin, "Thermo-elasto-plastic behaviour of a metal-matrix composite Al-6061/SiC and the effect of a precipitate-free zone around the reinforcement," Journal of Materials Processing Technology 1995; 55(3-4): 261-267. https://doi.org/10.1016/0924-0136(95)02016-0

[16] Y. Peng, H. Zhao, J. Ye, M. Yuan, L. Tian, Z. Li, Z. Wang, and J. Chen, "Multiscale 3D finite element analysis of aluminum matrix composites with nano–micro hybrid inclusions," Composite Structures 2022; 288: 115425. https://doi.org/10.1016/j.compstruct.2022.115425

[17] T. H. Nam, G. Requena, and H.-P. Degischer, "Modelling and numerical computation of thermal expansion of aluminium matrix composite with densely packed SiC particles," Technische Mechanik-European Journal of Engineering Mechanics 2008; 28(3-4): 259-267.

[18] K. Almadhoni and S. Khan, "Evaluation of the effective thermal properties of aluminum metal matrix composites reinforced by ceramic particles," International Journal of Current Engineering and Technology 2015; 5(4): 2884-2897.

[19] R. Guzmán and E. H. Arroyo, "Influence of thermal residual stress on behaviour of metal matrix composites reinforced with particles," Journal of Physics: Conference Series 2016; 687(1): 012060. https://doi.org/10.1088/1742-6596/687/1/012060

[20] D. Carou, E. M. Rubio, and J. P. Davim, "Machinability of magnesium and its alloys: A review," in Traditional Machining Processes: Research Advances, J. P. Davim, Ed. Berlin, Heidelberg: Springer 2014; 133–152. https://doi.org/10.1007/978-3-662-45088-8_5

[21] G. Singh and N. Sharma, "Study on the influence of T4 and T6 heat treatment on the wear behavior of coarse and fine WC particulate reinforced LM28 Aluminium cast composites," Composites Part C: Open Access 2021; 4: 100106. https://doi.org/10.1016/j.jcomc.2021.100106

[22] E. Mirkoohi, "Thermo-mechanical modeling of thermal stress in metal additive manufacturing considering elastoplastic hardening," CIRP Journal of Manufacturing Science and Technology 2020; 28: 52-67. https://doi.org/10.1016/j.cirpj.2020.01.002

[23] Y.-L. Shen, "Combined effects of microvoids and phase contiguity on the thermal expansion of metal-ceramic composites," Materials Science and Engineering: A 1997; 237(1): 102-108. https://doi.org/10.1016/S0921-5093(97)00121-4

[24] R. Yuan, S. S. Singh, X. Liao, J. Oswald, and N. Chawla, "Fracture analysis of particulate metal matrix composite using X-ray tomography and extended finite element method (XFEM)," *Journal of Composites Science*, vol. 4, no. 2, Art. no. 62, 2020.

[25] A. R. K. A. Ali and M. A. Jawad, "Finite element analysis of metal matrix composite materials," Journal of University of Babylon for Engineering Sciences 2018; 26(5): 166-175.

[26] H. Wang, "Numerical simulation of the mechanical properties and fracture of SiCp/6061Al composite materials based on microstructure," Metals 2023; 13(6): 1016. https://doi.org/10.3390/met13061016

[27] B. Prasanth Kumar and S. Johoram Babu, "Microstructure based finite element analysis for deformation behavior of aluminum based metal matrix composites," International Journal of Engineering Research & Technology (IJERT) 2014; 3(3). https://doi.org/10.17577/IJERTV3IS031963
[28] W. Miller and F. Humphreys, "Strengthening mechanisms in particulate metal matrix composites," Scripta Metallurgica et Materialia 1991; 25(1): 33-38. https://doi.org/10.1016/0956-716X(91)90349-6
[29] J. F. Wu, M. S. Shephard, G. J. Dvorak, and Y. A. Bahei-El-Din, "A material model for the finite element analysis of metal matrix composites," *Composites Science and Technology*, vol. 35, no. 4, pp. 347–366, 1989.
[30] NASA Lewis Research Center, "Using CT Data in Finite-Element Models of MMC Components," NASA Tech Briefs 1998; 22(9).
[31] N. Chawla and K. Chawla, "What's new in finite element modeling of particle reinforced metal matrix composites," presented at the 2006 TMS Annual Meeting 2006.
[32] Gao, M., Guo, E., Chen, Z., Kang, H. and Wang, T., 2023. Revealing the role of micropore defects in tensile deformation of a B4Cp/Al composite using an actual three-dimensional model. *Journal of Materials Research and Technology*, *22*, pp.3146-3155, https://doi.org/10.1016/j.jmrt.2022.12.145.
[33] G. Y. Baaklini, "X-ray microtomography of ceramic and metal matrix composites," Materials Evaluation, vol. 53, no. 9, 1995.
[34] H. Zhang, K. Ramesh, and E. Chin, "Effects of interfacial debonding on the rate-dependent response of metal matrix composites," Acta Materialia 2005; 53(17): 4687-4700. https://doi.org/10.1016/j.actamat.2005.07.004
[35] M. Shakoor, M. Bernacki, and P.-O. Bouchard, "Ductile fracture of a metal matrix composite studied using 3D numerical modeling of void nucleation and coalescence," Engineering Fracture Mechanics 2018; 189: 110-132. https://doi.org/10.1016/j.engfracmech.2017.10.027
[36] S. A. Ponnusami, S. Turteltaub, and S. van der Zwaag, "Cohesive-zone modelling of crack nucleation and propagation in particulate composites," Engineering Fracture Mechanics 2015; 149: 170-190. https://doi.org/10.1016/j.engfracmech.2015.09.050
[37] Q. Meng and Z. Wang, "Prediction of interfacial strength and failure mechanisms in particle-reinforced metal-matrix composites based on a micromechanical model," Engineering Fracture Mechanics 2015; 142: 170-183. https://doi.org/10.1016/j.engfracmech.2015.06.001
[38] J. N. Dastgerdi, "Effects of particle clustering on the plastic deformation and damage initiation of particulate reinforced composite utilizing X-ray CT data and finite element modeling," Composites Part B: Engineering 2018; 153: 57-69. https://doi.org/10.1016/j.compositesb.2018.07.027
[39] Y. Zhou, "Thermal damage in particulate-reinforced metal matrix composites," Journal of Engineering Materials and Technology 2001; 123(3): 251-260. https://doi.org/10.1115/1.1362675
[40] Y. Hou, "A crystal plasticity model for metal matrix composites considering thermal mismatch stress induced dislocations and twins," Scientific Reports 2021; 11(1): 16053.
[41] W. Chen, "One developed finite element model used in nano-layered flaky Ti2AlC MAX ceramic particles reinforced magnesium composite," Journal of Magnesium and Alloys 2024; 12(10): 4219-4228. https://doi.org/10.1016/j.jma.2023.04.009
[42] P. Sheng, "Effects of Particle Characteristics on the Fracture Behavior of A359/SiC Composites Based on a Micromechanical Method," Applied Composite Materials 2025; 1-25. https://doi.org/10.1007/s10443-025-10329-1
[43] Q. Wu, W. Xu, and L. Zhang, "Microstructure-based modelling of fracture of particulate reinforced metal matrix composites," Composites Part B: Engineering 2019; 163: 384-392. https://doi.org/10.1016/j.compositesb.2018.12.099
[44] L. Xi, "Enhanced manufacturing quality and mechanical performance of laser powder bed fused TiC/AZ91D magnesium matrix composites," Journal of Magnesium and Alloys 2025. https://doi.org/10.1016/j.jma.2024.12.012
[45] F. Hajializadeh and A. Ince, "Finite element–based numerical modeling framework for additive manufacturing process," Material Design & Processing Communications, vol. 1, no. 1, Art. no. e28, 2019.
[46] R. Sepasdar, A. Karpatne, and M. Shakiba, "A data-driven approach to full-field nonlinear stress distribution and failure pattern prediction in composites using deep learning," Computer Methods in Applied Mechanics and Engineering, vol. 397, Art. no. 115126, 2022.
[47] U. Bhandari, Y. Chen, H. Ding, C. Zeng, S. Emanet, P. R. Gradl, and S. Guo, "Machine-learning-based thermal conductivity prediction for additively manufactured alloys," Journal of Manufacturing and Materials Processing 2023; 7(5): 160. https://doi.org/10.3390/jmmp7050160 .
[48] M. Agarwal, P. Pasupathy, X. Wu, S. S. Recchia, and A. A. Pelegri, "Multiscale computational and artificial intelligence models of linear and nonlinear composites: A review," Small Science 2024; 4(5): 2300185. https://doi.org/10.1002/smsc.202300185
[49] ASM Handbook Committee, Properties and Selection: Nonferrous Alloys and Special-Purpose Materials, ASM Handbook, vol. 2, ASM International, Materials Park, OH, USA 1990. https://doi.org/10.31399/asm.h

b.v02.9781627081627
[50] M. M. Avedesian and H. Baker, Eds., ASM Specialty Handbook: Magnesium and Magnesium Alloys. Materials Park, OH, USA: ASM International 1999.
[51] M. Bauccio, Ed., ASM Metals Reference Book, 3rd ed. Materials Park, OH, USA: ASM International 1993.